The Formation and Stability of the [FePy$_3$Cl$_3$]·Py Clathrate in the Pyridine–Iron(III) Chloride System: Phase Diagram and Solid–Gas Equilibria Study

ANDREW G. OGIENKO*, ELISSA A. UKRAINTSEVA, TATYANA A. CHINGINA, VLADISLAV YU. KOMAROV and ANDREY YU. MANAKOV
Nikolaev Institute of Inorganic Chemistry SB RAS, Ac. Lavrentyev ave. 3, Novosibirsk 630090, Russian Federation

Abstract

The phase diagram of the pyridine–iron(III) chloride system has been studied for the 223–423 K temperature and 0–56 mass-% concentration ranges using differential thermal analysis (DTA) and solubility techniques. A solid with the highest pyridine content formed in the system was found to be an already known clathrate compound, [FePy$_3$Cl$_3$]·Py. The clathrate melts incongruently at 346.9 ± 0.3 K with the destruction of the host complex: [FePy$_3$Cl$_3$]·Py$_{(solid)}$ = [FePy$_2$Cl$_3$]$_{(solid)}$ + liquor. The thermal dissociation of the clathrate with the release of pyridine into the gaseous phase (TGA) occurs in a similar way: [FePy$_3$Cl$_3$]·Py$_{(solid)}$ = [FePy2Cl$_3$]$_{(solid)}$ + 2 Py$_{(gas)}$. Thermodynamic parameters of the clathrate dissociation have been determined from the dependence of the pyridine vapour pressure over the clathrate samples versus temperature (tensimetric method). The dependence experiences a change at 327 K indicating a polymorphous transformation occurring at this temperature. For the process $\frac{1}{2}$[FePy$_3$Cl$_3$]·Py$_{(solid)}$ = $\frac{1}{2}$[FePy$_2$Cl$_3$]$_{(solid)}$ + Py$_{(gas)}$ in the range 292–327 K, $\Delta H_{298}^0 = 70.8 \pm 0.8$ kJ/mol, $\Delta S_{298}^0 = 197 \pm 3$ J/(mol K), $\Delta G_{298}^0 = 12.2 \pm 0.1$ kJ/mol; in the range 327–368 K, $\Delta H_{298}^0 = 44.4 \pm 1.3$ kJ/mol, $\Delta S_{298}^0 = 116 \pm 4$ J/(mol K), $\Delta G_{298}^0 = 9.9 \pm 0.3$ kJ/mol.

Introduction

Werner clathrates is an important class of supramolecular materials [1–3]. Most studies accomplished so far were devoted to Werner clathrates of the general formula [MA$_4$X$_2$]·xG, where M is a metal(II) cation, A is a neutral ligand such as pyridine, X is a monovalent anionic group, and G is a guest component. One example of such inclusion compounds is a series of [MPy$_4$X$_2$]·2Py clathrates [4–6], where four molecules of pyridine form a part of the host complex while the other two molecules of pyridine are included in the host lattice as a guest. The clathrate nature of these compounds was illustrated by replacing the guest pyridine with other organic components [7]. Several series of the compounds were thoroughly studied to elucidate their thermal and thermodynamic properties, and how these properties change upon variation of the host components and the guest [8–10]. Much less is known about clathrates formed by molecular metal(III) complexes. Our literature search revealed only few compounds of general formula [MA$_3$X$_3$]·nG (Table 1). With pyridine as A, the

most typical host to guest molar ratio is 1:1 and the guest component is pyridine. The 1:2 host to guest molar ratio is observed with smaller guest molecules of acetonitrile, but the same ratio is observed with bulky pyridine and toluene in [TaPy$_3$Cl$_3$]·Py·MePh [11]. With 4-methylpyridine as A, four listed compounds fall into two groups differing in their stoichiometry, with host to guest molar ratio of 1:^{1}/$_2$ and 1:^{3}/$_2$; the guest component is 4-methylpyridine. The listed inclusion compounds were characterized structurally but almost no physicochemical studies of this type of clathrates have been reported. Systematic determinations of the clathrate formation conditions and real stoichiometry have not been carried out as well. The lack of this information made it difficult a substantial comparison of this new group of inclusion compounds with the well studied [MA$_4$X$_2$]·xG compounds.

The clathrate [FePy$_3$Cl$_3$]·Py is a typical representative of the group of clathrates with the host to guest ratio 1:1. Two polymorphous modifications of this compound (phase transition temperature 237 K) were found by Januszczyk et al. [12]. The low-temperature (here and there the phase I) modification was studied with single-crystal XRD analysis (190 K, sp. group C222$_1$,

*Author for correspondence: E-mail: ogienko@che.nsk.su

Table 1. Known clathrates of [MA₃X₃] complexes

Clathrate	Sp. group/ syngony	Unit cell parameters, A	*	Reference
[FePy$_3$Cl$_3$]·Py	C222$_1$	$a = 8.861$, $b = 16.712$, $c = 14.280$; $V = 2114.6$ A^3		[13]
[TiPy$_3$Cl$_3$]·Py	C222$_1$	$a = 17.002$, $b = 8.910$, $c = 14.482$; $V = 2193.9$ A^3		[14]
[TaPy$_3$Cl$_3$]·Py	C222$_1$	$a = 8.719$, $b = 17.042$, $c = 14.474$; $V = 2168.6$ A^3	√	[11]
[CrPy$_3$(NO$_2$)$_2$(NO)]·Py	Pnna	$a = 19.148$, $b = 10.101$, $c = 12.345$; $V = 2387.7$ A^3		[15]
[AlPy$_3$(N$_3$)$_3$]·Py	P2$_1$cn	$a = 10.645$, $b = 11.983$, $c = 18.688$; $V = 2383.8$ A^3		[16]
[TaPy$_3$Cl$_3$]·Py·MePh	P2$_1$/n, $\beta = 93.96°$	$a = 8.642$, $b = 18.750$, $c = 14.916$; $V = 2406.2$ A^3	√	[11]
[TiPy$_3$Cl$_3$]·2MeCN	C2/c, $\beta = 116.74°$	$a = 19.598$, $b = 11.009$, $c = 11.937$; $V = 2300.0$ A^3		[17]
[TcPy$_3$Cl$_2$(NO)]·2MeCN	C2/c, $\beta = 116.58°$	$a = 19.182$, $b = 10.873$, $c = 11.937$; $V = 2226.4$ A^3		[18]
[Cr(4-MePy)$_3$Cl$_3$]·1/2 4-MePy	monoclinic, $\beta = 96.52°$	$a = 8.543$, $b = 17.431$, $c = 15.840$; $V = 2343.5$ A^3	√	[19]
[Mo(4-MePy)$_3$Cl$_3$]·1/2 4-MePy	P2$_1$/n, $\beta = 95.80°$	$a = 8.595$, $b = 17.472$, $c = 15.911$; $V = 2377.2$ A^3	√	[19]
[Mo(4-MePy)$_3$Br$_3$]·1/2 4-MePy	P2$_1$/n, $\beta = 96.26°$	$a = 8.721$, $b = 17.827$, $c = 16.172$; $V = 2499.3$ A^3	√	[20]
[Cr(4-MePy)$_3$Br$_3$]·^{3}/$_2$ 4-MePy	monoclinic, $\beta = 101.40°$	$a = 8.730$, $b = 17.590$, $c = 16.370$; $V = 2464.2$ A^3	√	[21]

*The mark "√" means that the [MA$_3$X$_3$] host complex exists and its crystal structure is known.

$a = 8.861$ Å, $b = 16.712$ Å, $c = 14.280$ Å; $V = 2114.6$ Å^3), while for the high-temperature (here and there the phase II) modification only unit cell parameters were measured (290 K, $a = 4.745$ Å, $b = 14.395$ Å, $c = 7.816$ Å, $\beta = 93.93°$, $V = 535.7$ Å^3) [13]. In this work we elucidate dissociation behaviour and outline thermal and thermodynamic stability of the clathrate. Phase diagram of the pyridine–iron(III) chloride system in the clathrate formation region and thermodynamic parameters of the [FePy$_3$Cl$_3$]·Py clathrate dissociation are reported.

Experimental

Preparations

All preparations were done in a dry box desiccated with P$_2$O$_5$. The [FePy$_3$Cl$_3$]·Py was prepared by adding the anhydrous FeCl$_3$ (1.3 g, 8 mmol) to the excess of pyridine (10 ml, analytically pure grade, b.p. 388.2–388.7 K (cf. 388.5 K from literature)). The mixture was stirred and heated till a transparent red–brown solution formed. Red–brown crystals of the clathrate grew after the solution was left to cool down. The crystals were unstable in air and, therefore, were kept in a desiccator under thin layer of pyridine. When necessary, the crystals were dried with a piece of the blotting paper. *Anal. Calcd.* for [FePy$_3$Cl$_3$]·Py (mass%): Fe, 11.67; Py, 66.11. *Found*: Fe, 11.44(3); Py, 65.1(7).

Fe(III) was determined by a reverse titration with 0.04 M CuSO$_4$ solution of the excess of 0.02 M EDTA remaining after binding the Fe(III) cation, using pyrocatechin violet as an indicator, the maximum error in iron content being 1.5%. Pyridine was determined potentiometrically by reverse titration with 0.04 M KOH solution of the excess of 0.02 M nitric acid remaining after the neutralization of the pyridine base. The titration by literature technique revealed that presence of Fe(III) results into lowering of pyridine content. To avoid iron influence it was masked by addition of the theoretical amount of NaF (up to 1:6 Fe(III):F$^-$ molar ratio). This technique proved to give satisfactory results on titration of samples containing pyridine and FeCl$_3$ in molar ratio 1:3–1:4, the maximum error in pyridine content being 1.8%. Three or more determinations were performed in each case.

Phase diagram determination

A variety of samples differing in the pyridine to iron(III) chloride ratio were sealed in glass ampoules and studied with DTA technique. Samples with high concentration of pyridine were prepared by mixing neat pyridine and the [FePy$_3$Cl$_3$]·Py clathrate in various proportions. Samples with lower pyridine content were produced by a controlled dissociation of the grinded crystals of the clathrate in a desiccator with P$_2$O$_5$ (the composition was calculated from the mass loss and confirmed with the analysis of the samples for Fe). The ampoules with the samples were equilibrated at room temperature from several days to 4 months and then thermal curves were recorded for each of the ampoules. The temperatures of the phase transitions and approximate values of the corresponding thermal effects were determined from endothermal effects on the DTA thermograms. The accuracy of the temperature measurements was 0.5 K and the heating rate was 1.0 degree/min.

The solubility of the clathrate in pyridine (liquidus curve) was studied in the 293–353 K temperature range. Under a required temperature, the crystals of [FePy$_3$Cl$_3$]·Py were equilibrated with liquid pyridine. After the equilibrium between the solid and liquor was attained, a portion of the liquid phase was taken with a pre-heated pipette and analysed for the Fe content. It was determined in trial and error procedure that the system is in equilibrium if the composition of the liquid remained unchangeable for 3–4 h. In the 293–313 K temperature range, the approach to a required temperature was accomplished both from lower and from higher temperature.

Thermal decomposition processes were studied on a Q-derivatograph under quasi-equilibrium conditions

[22] using different sample holders. The sample mass was about 100 mg, the rate of the mass loss was 0.16 mg/min.

Strain experiments

The pyridine vapour pressure over the clathrate was measured by the static tensimetric method using a glass membrane null-manometer [23–25]. In a dry box, large red–brown crystals of the [FePy$_3$Cl$_3$]·Py clathrate were crushed and placed into the reaction vessel. The reaction vessel was evacuated for a shot time and sealed. The membrane sensitivity was 0.05–0.1 Torr, the thermo-statting and temperature measurement accuracy was 0.05 K. Two sets of measurements were carried out in the 292–368 K range. The process of dissociation of the clathrate was well reversible; the equilibrium vapour pressure established in several hours or faster. The $P(T)$ experimental data were approximated by the linear equation log $(P/\text{Torr}) = A - B/(T/\text{K})$, with the coeffi-cients A and B refined by a least-squares technique.

Results

Thermal dissociation of the compound

The [FePy$_3$Cl$_3$]·Py clathrate became unstable at lower temperatures when pyridine pressure is low (plate crucible), and stage which correspond to the reaction (1) can be separated. In the case of closed and conic crucibles, the pyridine pressure is high and the clathrate is stable to higher temperatures and then melts with decomposition.

Thermal decomposition of the [FePy$_3$Cl$_3$]·Py clath-rate in air flow under quasi-isobaric, quasi-isothermal heating conditions (Figure 1) indicates that a change of the evolving pyridine does not cause any changes in the manner of the clathrate decomposition, which follows the reaction:
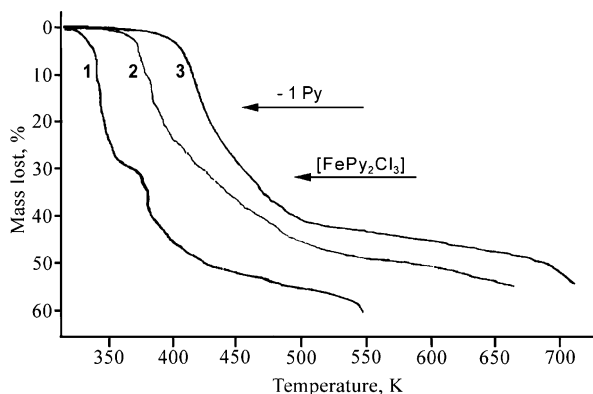
$$[\text{FePy}_3\text{Cl}_3] \cdot \text{Py}_{(\text{solid})} = [\text{FePy}_2\text{Cl}_3]_{(\text{solid})} + 2\text{Py}_{(\text{gas})} \quad (1)$$

Figure 1. Mass loss curves for [FePy$_3$Cl$_3$]·Py recorded under quasi-equilibrium conditions. Sample mass: 150 mg; $q = 0.16$ mg/min; sample holders: 1, plate; 2, closed; 3, conic crucibles.
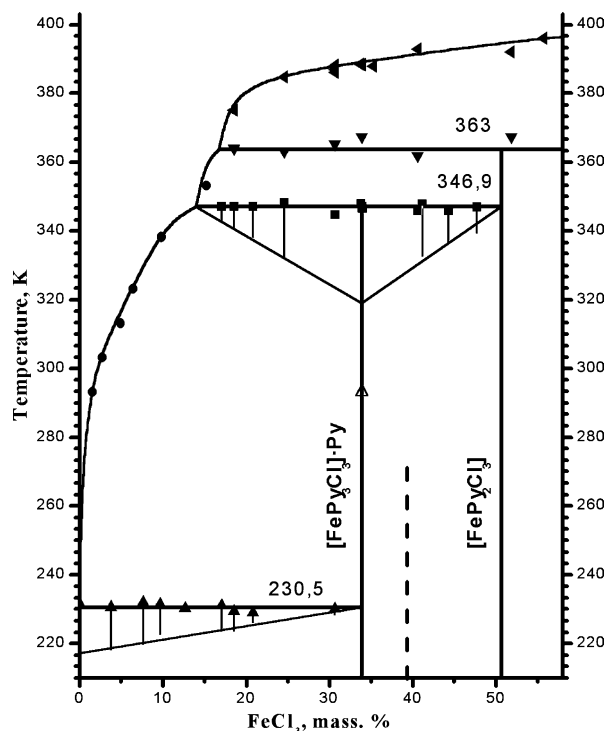

Figure 2. Phase diagram of the pyridine–FeCl$_3$ system. Designations: Δ, analitical data (calcd. for [FePy$_3$Cl$_3$]·Py (%): Fe, 11.67; Py, 66.11; found: Fe, 11.44 ± 0.03; Py, 65.1 ± 0.7 (experimental errors are given for the probability level of 95 %)); ▲, DTA data defining the eutectics Py$_{(\text{solid})}$ + liquor + [FePy$_3$Cl$_3$]·Py$_{(\text{solid})}$; ■, DTA data defining the peritectics liquor + [FePy$_3$Cl$_3$]·Py$_{(\text{solid})}$ + [FePy$_2$Cl$_3$]$_{(\text{solid})}$; ▼, DTA effects arising from incongruent melting of [FePy$_2$Cl$_3$]; ◄, DTA data defining the liquidus curve; ●, data on solubility of the clathrate in pyridine (define liquidus curve).
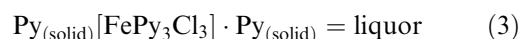
Remarkably, the dissociation of the clathrate phase is accompanied by the dissociation of the host complex [FePy$_3$Cl$_3$].

Phase diagram of the FeCl$_3$–Py system

Figure 2 shows the phase diagram of the FeCl$_3$–pyridine system in the clathrate formation region. The coordi-nates of the experimental points defining the liquidus curve are listed in Table 2. The compound with the highest content of pyridine forming in the system has four moles of pyridine per one mole of FeCl$_3$; according to previous studies [13] it has a clathrate structure with one of pyridines included as the guest: [FePy$_3$Cl$_3$]·Py. The clathrate is stable up to 346.9 K; at further heating it melts incongruently according to the equation:

$$[\text{FePy}_3\text{Cl}_3] \cdot \text{Py}_{(\text{solid})} = [\text{FePy}_2\text{Cl}_3]_{(\text{solid})} + \text{liquor} \quad (2)$$

The eutectics

$$\text{Py}_{(\text{solid})}[\text{FePy}_3\text{Cl}_3] \cdot \text{Py}_{(\text{solid})} = \text{liquor} \quad (3)$$

is degenerated and its temperature (230.5 K) is very close to the melting point of neat pyridine (231.6 K). A phase transition observed at 363 K was attributed to

Table 2. Coordinates of the liquidus curve experimental points in the title system

T (K)	FeCl₃, mass-%	Method	Phases in equilibrium
231.6	0	DTA	1 + Py (solid)
293.2	1.54 ± 0.02; 1.55 ± 0.07*	Solubility	1 + [FePy₃Cl₃]·Py
303.2	2.74 ± 0.06; 2.76 ± 0.09*	Solubility	1 + [FePy₃Cl₃]·Py
313.2	4.76 ± 0.06; 4.97 ± 0.08*	Solubility	1 + [FePy₃Cl₃]·Py
323.2	6.44 ± 0.09	Solubility	1 + [FePy₃Cl₃]·Py
338.2	9.80 ± 0.04	Solubility	1 + [FePy₃Cl₃]·Py
353.2	15.2 ± 0.3	Solubility	1 + [FePy₃Cl₃]·Py
375.2	18.5	DTA	1 + X
384.7	24.57	DTA	1 + X
387.1	30.66	DTA	1 + X
392.8	40.6	DTA	1 + X
392.0	51.79	DTA	1 + X
396.0	55.71	DTA	1 + X

*In these cases the equilibrium was achieved from the lower and the higher temperature.

the incongruent melting of the [FePy₂Cl₃] complex (the highest specific thermal effects were observed for the samples having this composition). Phase transition of the [FePy₃Cl₃]·Py clathrate compound at 237 K [12] has not been observed on experimental thermogrames probably due to low values of corresponding heat effects.

Pyridine vapour pressure over the [FePy₃Cl₃]·Py compound

The temperature dependence of the pyridine vapour pressure over the [FePy₃Cl₃]·Py clathrate is shown in Figure 3. The dependence experiences two bends, at 327 and 346 K. The bend at 327 K indicates polymorphous transformation of the clathrate, and the bend at 346 K corresponds well to the incongruent melting point of this compound. Therefore, there are three segments where the
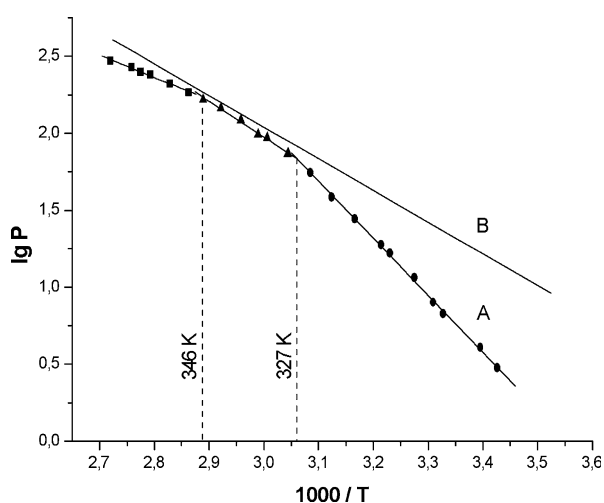

Figure 3. Temperature dependence of the pyridine vapour pressure over the [FePy₃Cl₃]·Py clathrate. log *P*-1000/*T* coordinates (*P*/Torr, *T*/K).

pressure logarithm is a linear function of reverse temperature. In the studied 292–368 K temperature range the segments are described by the following equations:

Segment 1 (292 − 327 K)
$$\log P = (13.15 \pm 0.14) - (3698 \pm 44)/T \, (10 \text{ exp. points})$$
(4)

Segment 2 (327 − 346 K)
$$\log P = (8.94 \pm 0.20) - (2320 \pm 68)/T \, (7 \text{ exp. points})$$
(5)

Segment 3 (346 − 368 K)
$$\log P = (6.42 \pm 0.16) - (1450 \pm 59)/T \, (6 \text{ exp. points})$$
(6)

The Equations (4–6) define pyridine vapour pressure over a low-temperature clathrate modification (the phase II) , over high-temperature clathrate modification (here and there the phase III) and over saturated solution of [FePy₂Cl₃] in pyridine, respectively. Thermodynamic parameters calculated from the found *P(T)* dependence for the clathrate dissociation process are listed in Table 3.

Discussion

The phase diagram of the studied system (Figure 2) reveals the temperature-concentration stability region of the [FePy₃Cl₃]·Py clathrate compound. At the same time, the [FePy₃Cl₃] host complex does not appear as a thermodynamically stable solid in the system. The removal of the guest pyridine from the clathrate phase causes dissociation of the host complex to a compound with lower pyridine content, [FePy₂Cl₃] (Equation 1). A similar result (Equation 3) is observed from the TGA experiments (Figure 2). Therefore, the molecules of *mer*-[FePy₃Cl₃] exist only in the clathrate phase and cannot create a thermodynamically stable guest-free solid. Thus we see that, depending on the type of paking in the host-guest system, the host molecules themselves undergo a substantial rearrangement, i.e. the non-bonded intermolecular interactions affect the conformation of the host molecules. Earlier, similar observations were made for some [MA₄X₂]·*x*G clathrate compounds and this phenomenon was referred as "contact stabilization" of host complex molecules in a supramolecular clathrate matrix [8, 9, 26–28], by analogy with the term "contact stabilization isomerism" introduced by Zorkii [29] to describe the coexistence in a homomolecular crystal of more than one molecular conformation, which also determined by the packing factor. In other words the host molecule does not exist at all in the absence of contacts with the guests molecules, i.e. without their non-bonded "support". Therefore, the contribution of non-valent interactions which are responsible for retaining of the guest inside the solid phase is comparable in this system to a contribution of the chemical coordination bonds in the host complex.

Table 3. Thermodynamic parameters of dissociation of two polymorphs of the studied [FePy$_3$Cl$_3$]·Py clathrate (for the reaction $\frac{1}{2}$[FePy$_3$Cl$_3$]·Py$_{(solid)}$ = $\frac{1}{2}$[FePy$_2$Cl$_3$]$_{(solid)}$ + Py$_{(gas)}$) and some known Werner clathrates

Compound	T-range	ΔH^0, kJ/mol	ΔS^0_{298}, J/(mol K)	ΔG^0_{298}, kJ/mol	Reference
[FePy$_3$Cl$_3$]·Py	292–327	70.8 ± 0.8	197 ± 3	12.2 ± 0.1	This work.
	327–346	44.4 ± 1.3	116 ± 4	9.9 ± 0.3	
[CuPy$_4$(NO$_3$)$_2$]·2Py	304–333	74.6	197	15.9	[32]
	333–378	57.2	145	14.1	
[NiPy$_4$(NO$_3$)$_2$]·2Py	293–347	64.6	168	14.4	[32]
	347–374	57.2	146.9	13.4	

The thermodynamic parameters for dissociation of the studied [FePy$_3$Cl$_3$]·Py clathrate are comparable to analogous parameters for previously studied [MPy$_4$X$_2$]·xPy compounds (some are listed in Table 3). It is interesting that the increasing charge of the M central cation does not make a significant difference in the thermodynamic stability of the resulting clathrate phases. This conclusion illustrates further similarity between clathrate compounds of M(II) and M(III) complexes.

From the comparison of thermodynamic parameters of low-temperature (phase II) and high-temperature (phase III) polymorphous modifications of the studied and previously known clathrates (Table 3), it is clearly seen that the transition into high-temperature modifications occur at the expense of significant entropy profit while the resulting change in free energy is not very big. This implies an additional disorder in the high-temperature modifications of the clathrates. Detailed studies of polymorphous transitions in [CdPy$_4$(NO$_3$)$_2$]·2Py [30] and [CuPy$_4$(NO$_3$)$_2$]·2Py [31] showed that the appearance of the additional disorder in these clathrates at similar temperatures occurs due to increasing dynamics of weakly bonded nitrate groups. In the compound of this study the disorder may arise from increasing dynamics of the host molecules. The single-crystal XRD study of the high-temperature form of the clathrate (phase III) would be useful to elucidate these changes.

Conclusion

The first physicochemical study of a clathrate compound with M(III) Werner complex, [FePy$_3$Cl$_3$]·Py, was performed. The data obtained make it possible to conclude that the physicochemical properties of the studied [FePy$_3$Cl$_3$]·Py clathrate reveal similarity with some well-known Werner clathrates. The contribution of non-valent interactions to the overall stability of the clathrate phase is significant and favours the formation of the host [FePy$_3$Cl$_3$] complex molecules inside the clathrate matrix. The guest–free form of the host complex does not exist as a thermodynamically stable solid in the system studied. Therefore, the clathration process is a convenient, and may be the only, way to stabilize the [FePy$_3$Cl$_3$] complex in the solid phase due to the contact stabilization phenomenon. This study shows that inclusion phenomena may well be used to observe and to characterize other M(III) complexes which are not stable enough to exist in solvent-free forms.

References

1. J. Lipkowski: In J.L. Atwood, J.E.D. Davies, and D.D. MacNicol (eds.), *Inclusion Compounds* Vol. 1 Academic Press, London (1984), pp. 59–103.
2. J. Hanotier and P. Radzitzky: In J.L. Atwood, J.E.D. Davies and D.D. MacNicol (eds.), Inclusion Compounds Vol 1, Academic Press, London (1984), pp. 104–134.
3. D.V. Soldatov: *J. Incl. Phenom.* **48**, 3 (2004).
4. D.V. Soldatov and J. Lipkowski: *J. Struct. Chem.* **36**, 979 (1995).
5. D.V. Soldatov and J.A. Ripmeester: *Supramol. Chem.* **9**, 175 (1998).
6. D.V. Soldatov, G.D. Enright, J.A. Ripmeester, J. Lipkowski, and E.A. Ukraintseva: *J. Supramol. Chem.* **1**, 245 (2001).
7. D.V. Soldatov, Yu. A. Dyadin, J. Lipkowski, and A.G. Ogienko: *Mendeleev Commun.* **11** (1997).
8. Yu. A. Dyadin, D.V. Soldatov, V.A. Logvinenko, and J. Lipkowski: *J. Coord. Chem.* **37**, 63 (1996).
9. E.A. Ukraintseva, D.V. Soldatov, Yu. A. Dyadin, V.A. Logvinenko, and E.V. Grachev: *Mendeleev Commun.* 123 (1999).
10. E.A. Ukraintseva, D.V. Soldatov, and Yu. A. Dyadin: *J. Incl. Phenom.* **48**, 19 (2004).
11. F.A. Cotton, C.A. Murillo, and Xiaoping Wang: *Inorg. Chem. Acta* **245**, 115 (1996).
12. M. Januszczyk, J. Pietrzak, and A. Stecki: *Proc XXVII Meet. Pol. Phys. Soc.* M. Curie-Sklodowska Univ., Lublin, Poland 109 (1981).
13. A. Hoser, Z. Kaluski, M. Januszczyk, J. Pietrzak, and T. Glowiak: *Acta Crystallogr. Sect. C.* **39**, 1039 (1983).
14. R.K. Collins and M.G. Drew: *Inorg. Nucl. Chem. Lett.* **8**, 975 (1972).
15. C.M. Lukehart and J.M. Troup: *Inorg. Chim. Acta* **22**, 81 (1977).
16. R.A. Fischer, A. Miehr, H. Sussek, H. Pritzkow, E. Herdtweck, J. Muller, O. Ambacher, and T. Metzger: *Chem. Commun.* 2685 (1996).
17. S.I. Troyanov, A.I. Yanovsky, and Yu.T. Struchkov: *Koord. Khim.* **21**, 332 (1995).
18. S.S. Blanchard, T. Nicholson, A. Davison, W. Davis, and A.G. Jones: *Inorg. Chim. Acta* **244**, 121 (1996).
19. J.V. Brencic and I. Leban: *Z. Anorg. Allg. Chem.* **465**, 173 (1980).
20. J.V. Brencic, I. Leban, and M. Slokar: *Acta Crystallogr., Sect. B.* **36**, 698 (1980).
21. J.V. Brencic, and I. Leban: *Z. Anorg. Allg. Chem* **445**, 251 (1978).
22. V.A. Logvinenko, J. Paulik, and F. Paulik: *Kvaziravnovesnaja Termogravimetrija v Sovremennoj Neorganicheskoj Khimii*, Nauka, Novosibirsk (1989).

236

23. A.V. Suvorov: *Termodinamicheskaya khimiya paroobraznogo sostoyaniya. Tenzimetricheskiye issledovaniya geterogennykh ravnovesij,* pp. 46–51. Khimiya, Leningrad (1970) (in Russian).
24. V.B. Lazarev, J.H. Greenberg, and B.A. Popovkin: *Curr. Top. Mater. Sci* **1**, 657 (1978).
25. E.A. Ukraintseva, Yu. A. Dyadin, N.V. Kislykh, V.A. Logvinenko, and D. V. Soldatov: *J. Incl. Phenom.* **23**, 23 (1995).
26. Yu. A. Dyadin, and N.V. Kislykh: *Mendeleev Commun.* 134 (1991).
27. Yu. A. Dyadin: *Russ. J. Coord. Chem* **22**, 402 (1996).
28. V.A. Logvinenko, and D.V. Soldatov: *J. Thermal Anal.* **56**, 485 (1999).
29. P.M. Zorkii, and A.E. Razumaeva: *J. Struct. Chem.* **20**, 819 (1979).
30. D.V. Soldatov, B.A. Kolesov, J. Lipkowski, and Yu. A. Dyadin: *J. Struct. Chem.* **38**, 463 (1997).
31. D.V. Soldatov, G.D. Enright, J.A. Ripmeester, J. Lipkowski, and E.A. Ukraintseva: *J. Supramol. Chem.* **1**, 245 (2001).
32. D.V. Soldatov, E.A. Ukraintseva, V.A. Logvinenko, Yu. A. Dyadin, E.V. Grachev, and A. Yu. Manakov: *Supr. Chem* **12**, 237 (2000).